Supporting Information

Single-atom Ru catalyst for selective synthesis of 3-pentanone via ethylene hydroformylation

Tingting Qin,[a,b,+] Yaru Dang,[a,b,+] Tiejun Lin,[a,+] Bingbao Mei,[b,c] Bo Wu,[a,b] Xiao Li,[a,b] Shenggang Li,[a,d] Zheng Jiang,[e] Zhiyong Tang,[a] Liangshu Zhong*[,a,d] and Yuhan Sun*[,a,d]

[a] CAS Key Laboratory of Low-Carbon Conversion Science and Engineering, Shanghai Advanced Research Institute, Chinese Academy of Science (CAS), Shanghai 201210, PR China.

[b] University of the Chinese Academy of Science, Beijing 100049, PR China.

[c] Shanghai Institute of Applied Physics, Chinese Academy of Sciences, Shanghai 201800, PR China

[d] School of Physical Science and Technology, ShanghaiTech University, Shanghai 201210, PR China.

[e] Shanghai Synchrotron Radiation Facility, Zhangjiang National Lab, Shanghai Advanced Research Institute, Chinese Academy of Sciences, Shanghai 201210, PR China

[+] These authors contributed equally to this work.

[*] *Corresponding author*.

Corresponding authors at: CAS Key Laboratory of Low-Carbon Conversion Science and Engineering, Shanghai Advanced Research Institute, Chinese Academy of Sciences, Shanghai, 201210, PR China.

E-mail addresses: zhongls@sari.ac.cn (L. Zhong), sunyh@sari.ac.cn (Y. Sun).

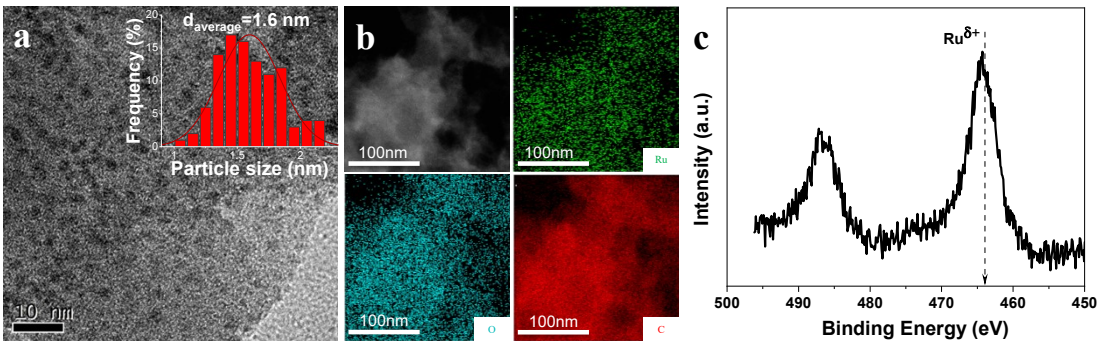

Figure S1. Electron microscopic characterization and Ru 3p spectra of fresh 3.3Ru NPs catalyst. (a) TEM image. (b) HAADF-STEM image and the corresponding EDX element mapping. (c) Ru 3p spectra.

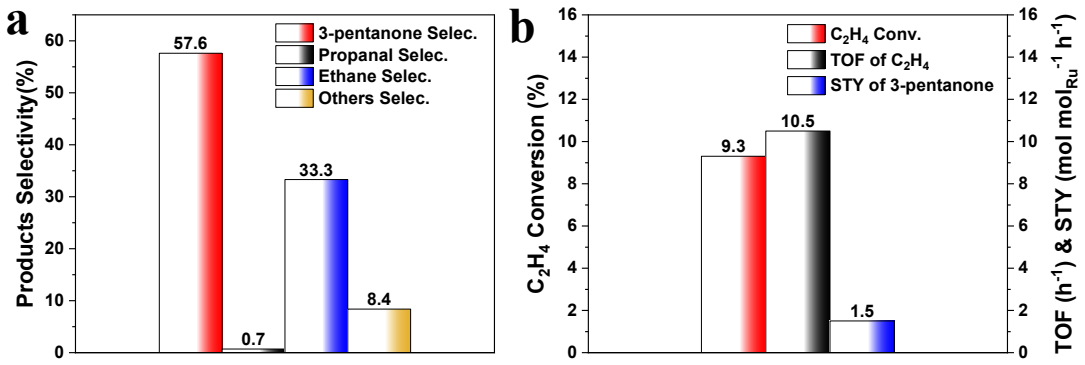

Figure S2. Catalytic performance of 3.3Ru NPs catalyst. (a) Selectivity; (b) TOF of C_2H_4 and STY of 3-pentanone. Reaction conditions: 1.5 g catalyst, 150 °C, 2000 mL $g_{cat.}^{-1}$ h^{-1}, 2 MPa and C_2H_4/CO/H_2=2:1:1.

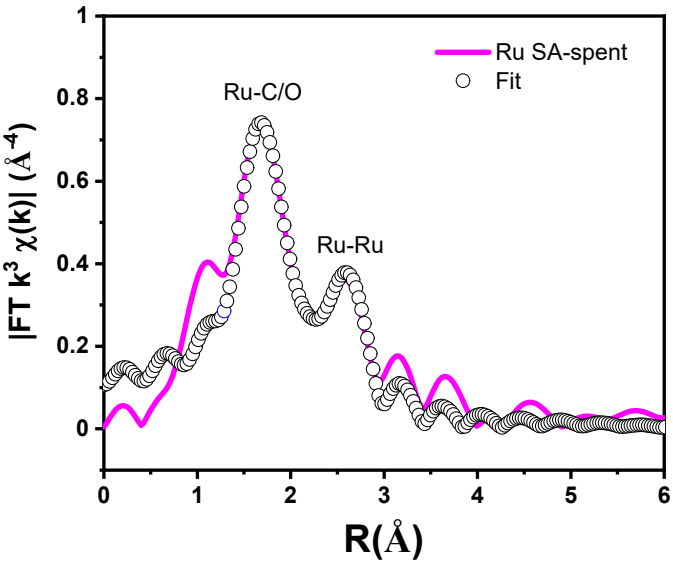

Figure S3. Fourier-transform EXAFS spectra of the spent Ru SA catalyst.

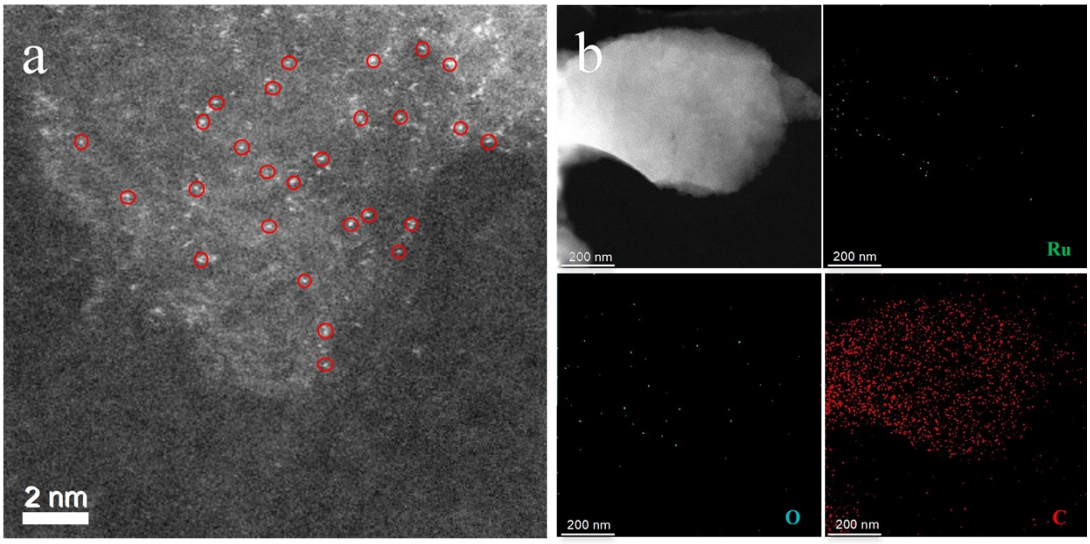

Figure S4 Electron microscopic characterization of spent Ru SA catalyst. (a) AC-HADDF-STEM image. (b) HAADF-STEM image and the corresponding EDX element mapping.

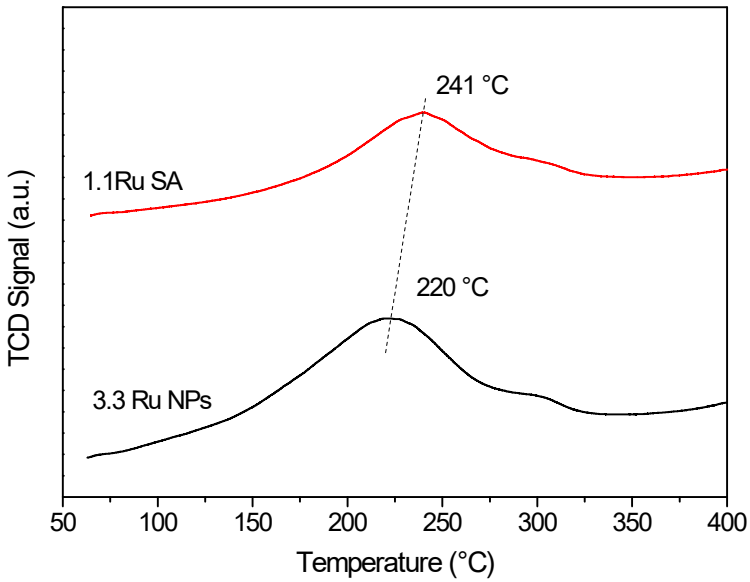

Figure S5 H_2-TPR results of fresh 1.1Ru SA and 3.3Ru NPs

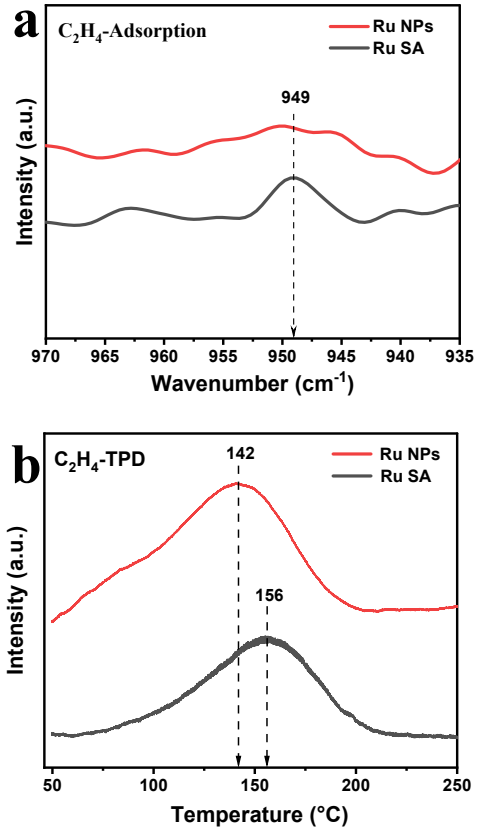

Figure S6. Ethylene adsorption study. a) In-situ DRIFTS spectra of ethylene adsorption collected after ethylene adsorption and vacuum desorption (30 min) at 50 °C. b) C_2H_4 temperature programmed desorption (C_2H_4-TPD).

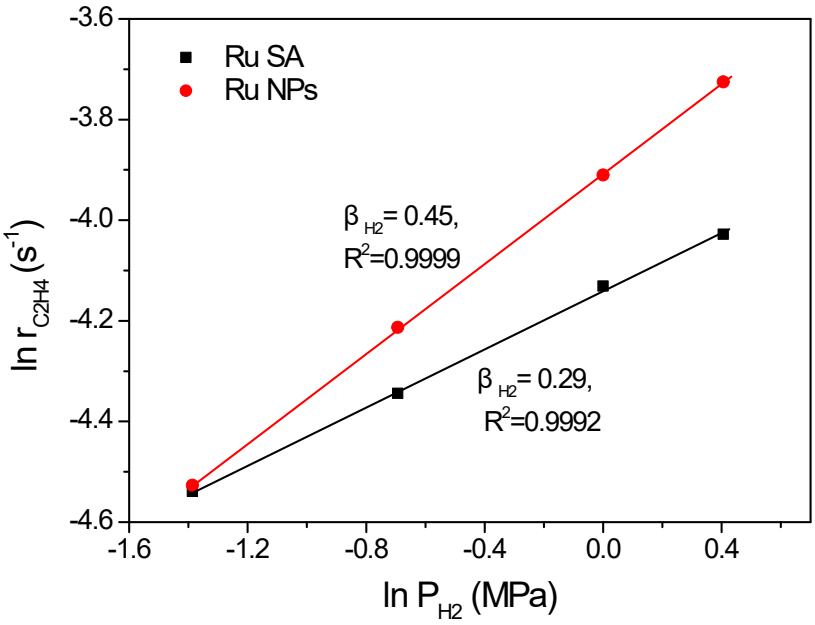

Figure S7 Dependence of conversion rate on partial pressure of H_2 over Ru SA and Ru NPs. Reaction conditions: 2 MPa, 150 °C, 12000 mL $g_{cat.}^{-1}$ h^{-1}.

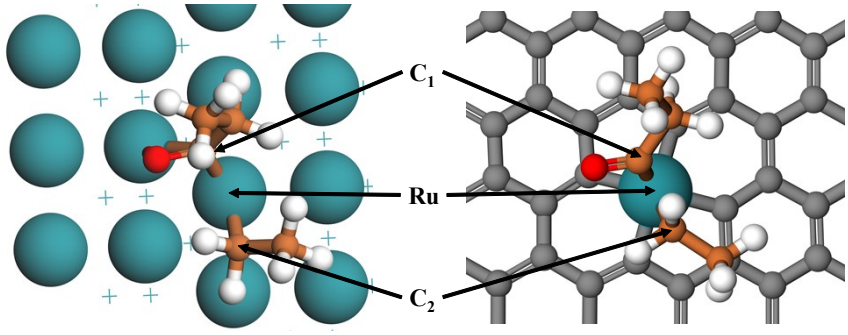

Figure S8. Transition state structures for 3-pentanone formation on Ru SA and Ru NPs catalysts. Ru NPs modeled by the Ru (101) slab model. Ru, O, H, C in AC and C in 3- pentanone are blue, red, white, gray and orange, respectively. The C in the C_2H_5CO* was marked as C1, and the C in the C_2H_5* was marked as C_2.

Table S1. Textural properties of various catalysts.

Samples	S_{BET} [a] (m^2/g)	S_{micro} [b] (m^2/g)	S_{micro}/S_{BET} (%)	V_T [c] (cm^3/g)	V_{micro} [b] (cm^3/g)	V_{micro}/V_T (%)	Pore size (nm)	Ru loading (wt%) [d]
AC	1275	725	56.9	0.67	0.38	56.7	2.1	-
Ru SA	1258	731	58.1	0.66	0.38	57.6	2.1	1.1

[a] S_{BET} is the specific surface area calculated by the Brunauer–Emmett–Teller (BET) method.

[b] Micropore area (S_{micro}) and micropore volume (V_{micro}) were determined according to the t-plot method.

[c] Total pore volume calculated as the amount of nitrogen adsorbed at a relative pressure (P/P_0) of 0.99.

[d] Measured by ICP-OES.

Table S2 Comparison of catalytic performance for 3-pentanone formation via heterogeneous ethylene hydroformylation over various supported catalysts.

Catalysts	metal loading (wt%)	T (℃)	P (MPa)	$C_2H_4/CO/H_2$	Activity (10^{-6} mol·min^{-1}·mol$_{metal}^{-1}$)	Selectivity (%)	References
Ru SA	1.1	150	2.0	2:1:1	99049	71.1	This work
Co/AC	10.0	120	3.0	1:1:1	16914	55.1	[1]
NiMo/carbon	13.1(Total)	290	1.0	1:1:1	80218	/	[2]
Ir/carbon	12.9	290	1.0	1:1:1	69541	/	[2]
Rh/AC	1.0	120	1.0	1:1:1	5145	/	[3]
Rh/AC	2.0	120	1.0	1:1:1	4116	/	[4-6]
Rh/AC	2.0	120	0.1	1:1:1	4116	/	[7]
Rh/AC	2.0	150	2.0	1:1:1	19 [a]	/	[8]
$NiMo/Al_2O_3$	11.9(Total)	290	1.0	1:1:1	Trace	/	[9]
$2\text{-}Rh\text{-}PPh_3/SiO_2$	2.0	110	0.5	1:1:1	/	3.7	[10]
Rh/C(C)	7.7	110	0.5	1:1:1	/	15	[10]
Rh/fibre	3.0	100	0.5	1:1:1	/	0.1	[10]
Rh/C(C)	5.0	173	0.5	1:1:1	/	trace	[11]
Co/ZnO	0.84	160	8.0	1:1:1	/	4	[12]
Co/La_2O_3	0.75	160	8.0	1:1:1	/	0.2	[12]
Co/MgO	0.96	160	8.0	1:1:1	/	0	[12]
$Ru_3(CO)_9(TPPMS)_3$ [b]	/	100	5.0	4.7:1:1	/	52.7 [c]	[13]
$Rh/2.9ReO_x\text{-}Al_2O_3$	0.23	120	0.1	1:1:1	/	0	[14]
$5\%Rh/Al_2O_3$	5.0	205	2.0	1:1:1	/	0	[15]
$0.5\%Rh\text{-}0.5\%Co/Al_2O_3$	1.0(Total)	205	2.0	1:1:1	/	0	[15]
$Rh_1Co_3/MCM\text{-}41$	2.72(Total)	180	0.1	1:1:1	/	0	[16]
$0.6Rh0.23Co/SiO_2$	0.83	180	1.0	1:1:1	/	0	[17]
Rh/SiO_2	5	150	0.1	1:1:1	/	0	[18]
$Ru\text{-}Co/SiO_2$	2.7(Total)	150	0.1	1:1:1	/	0	[19]
$5\text{-}Co(A)/SiO_2$	5.2	163	0.5	1:1:1	/	0	[20]
Rh/SiO_2	4.0	115	0.1	1:1:1	/	0	[21]

[a]: TOF:10^{-3} min^{-1}. [b]: Homogeneous catalytic system. [c]: Yield.

As shown in Table S2, the reported Ru SA catalyst in this work almost exhibited

the highest activity and selectivity than the state-of-the-art heterogeneous catalysts. It should be noted that most of the reported heterogeneous ethylene hydroformylation catalysts shows trace or negligible 3-pentanone selectivity.

Table S3. Catalytic performance comparison of various activated carbon supported catalysts.

Catalysts	C_2H_4 Conv. (%)	Selectivity (C%)					STY [d] (mol mol_{Ru}^{-1} h^{-1})
		Propanal [a]	3-Pentanone	Ethane	Aldol cond. [b]	Olig.[c]	
Ru SA	7.7	7.1	71.1	15.7	1.8	4.3	5.9
Rh/AC	5.1	0.8	42.4	46.2	8.8	1.9	0.5
Rh/AC [e]	8.7	5.8	45.4	32.1	16.2	0.4	1.9
Co/AC	1.2	0	0	85.7	0	14.3	0

Reaction conditions: 150 °C, 2 MPa, 2000 mL $g_{cat.}^{-1}$ h^{-1}, $C_2H_4/CO/H_2$=2:1:1 without reduction treatment. [a] Propanal: propanal and propanol; [b] Aldol cond.: Aldol condensation of propanal, mainly including 2-methyl-2-pentenal, 2-methylvaleraldehyde, 2-methyl-1-pentanol and propyl propionate; [c] Olig.: Ethylene oligomers and the possible isomerization and hydrogenation products. [d] The STY was calculated as the molar amount of 3-pentanone produced per mole of Ru per hour. [e] $C_2H_4/CO/H_2$=1:1:1.

Table S4. Comparison of catalytic performance for various supported Ru-based catalysts.

Catalysts	C_2H_4 Conv. (%)	Selectivity (C%)					STY [d] (mol mol_{Ru}^{-1} h^{-1})
		Propanal [a]	3-Pentanone	Ethane	Aldol cond. [b]	Olig.[c]	
Ru SA	9.6	4.9	56.0	31.3	0.9	7.0	4.9
Ru/Al_2O_3	1.3	61.8	16.0	17.0	0.0	5.1	0.1
Ru/SiO_2	4.1	37.6	21.8	38.1	0.9	1.7	0.5

Reaction conditions: 150 °C, 2 MPa, 2628 mL $g_{cat.}^{-1}$ h^{-1}, $C_2H_4/CO/H_2$=1:2.5:2.5 without reduction treatment. [a] Propanal: propanal and propanol; [b] Aldol cond.: Aldol condensation of propanal, mainly including 2-methyl-2-pentenal, 2-methylvaleraldehyde, 2-methyl-1-pentanol and propyl propionate; [c] Olig.: Ethylene oligomers and the possible isomerization and hydrogenation products. [d] The STY was

calculated as the molar amount of 3-pentanone produced per mole of Ru per hour.

Table S5. XANES analysis and EXAFS fitting results of spent Ru SA catalyst.

Coordination	CN	R(Å)	$\sigma^2\times10^{-3}$(Å^2)	ΔE(eV)	R-factor
Ru-O/C	3.3	2.14	3.2	14.0	0.95%
Ru-Ru	3.4	2.63	9.0	4.7	

R: distance; CN: coordination umber; σ^2: Debye-Waller factor; ΔE: correction to the photoelectron energy origin.

Table S6 The results of chemical information between the calculated species and catalytic sites.

Sample	Species	rC$_1$Ru (Å)	rC$_2$Ru (Å)	rORu (Å)	rC$_1$C$_2$ (Å)	∠C$_1$RuC$_2$ (º)
Ru SA	IS	2.052	2.221	2.732	2.638	76.1
	TS	2.013	2.485	2.618	2.142	55.7
	FS	2.228	3.305	2.135	1.51	22.5
Ru NPs	IS	3.119	3.472	3.231	4.975	97.9
	TS	2.102	2.224	2.896	2.789	80.2
	FS	2.18	3.2	2.169	1.52	24.6

r: distance; ∠: bond angle.

For the DFT calculation, the C atom in C_2H_5CO* is denoted as C1, and C atom in C_2H_5* is denoted as C2. As for Ru SA, the C_2H_5CO* and C_2H_5* are simultaneously adsorbed on the Ru atom. The distance for C1-Ru, C2-Ru and C1-C2 is 2.052Å, 2.221Å, and 2.638Å, respectively. After the formation of 3-pentanone, the C1 atom and the O atom are simultaneously coordinated to the Ru atom. The bond length for C1-Ru is 2.228 Å and that for O-Ru is 2.135 Å, respectively, and the C1-C2 bond length is 1.510 Å. The distance of C1-C2 for the transition state structure is 2.142Å.

The active site of NPs catalysts is composed of 5 Ru atoms. After 3-pentanone is formed, it is coordinated on the central Ru atom. Before reaction, C_2H_5CO* and C_2H_5* are adsorbed on the Ru atoms on both sides, respectively. The distance of C1-Ru, C2-Ru and C1-C2 is 3.119Å, 3.472Å and 4.975Å, respectively. After the formation of 3-pentanone, the C1 atom is coordinated to the middle Ru atom with 2.180Å of the bond length, and the C1-C2 bond length is 1.520Å. The distance of C1-C2 for the transition state structure is 2.789Å.

References

[1] Song, X., Ding, Y., Chen, W., Dong, W., Pei, Y., Zang, J., Yan, L., Lu, Y., Formation of 3-pentanone via ethylene hydroformylation over Co/activated carbon catalyst. *Appl. Catal. A: Gen.*, 2013, **452**, 155-162.

[2] Vit, Z., Portefaix, J.L., Zdrazil, M., Breysse, M., Ketones formation during ethylene hydroformylation over sulfided Rh, Ir and NiMo carbon-supported catalysts. *Catal. Lett.*, 1995, **32**, 55-59.

[3] Takahashi, N., Takabatake, Y., Sakagami, H., Imizu, Y., Okazaki, N., Tada, A., Effects of chlorine on formation of 3-pentanone during ethene hydroformylation over Rh/active-carbon catalyst. *J. Catal.*, 1996, **159**, 491-495.

[4] Takahashi, N., Takeyama, T., Yanagibashi, T., Takada, Y., Comparison of Pentan-3-One Formation with Propionaldehyde Formation during Ethylene Hydroformylation over Rh Active-Carbon Catalyst. *J. Catal.*, 1992, **136**, 531-538.

[5] Takahashi, N., Arakawa, H., Kano, A., Fukagawa, Y., Asao, K., Pentan-3-one formation from ethylene, carbon-monoxide and hydrogen over rhodium supported on active-carbon. *Chem. Lett.*, 1990, **19**, 205-208.

[6] Claridge, J.B., Green, M.L.H., Tsang, S.C., York, A.P.E., Conversion of propanal to pentan-3-one using lanthanide oxides. *J. Chem. Soc. Faraday Trans.*, 1993, **89**, 1089-1094.

[7] Takahashi, N., Sato, Y., Uchiumi, T., Ogawa, K., Unusual effects of the reaction temperature on the catalystic activity of Rh/active-carbon for ethylene hydroformylation. *Bull. Chem. Soc. Jpn.*, 1993, **66**, 1273-1278.

[8] Sakagami, H., Ohta, N., Endo, S., Harada, T., Takahashi, N., Matsuda, T., Location of active sites for 3-pentanone formation during ethene hydroformylation on Rh/active-carbon catalysts. *J. Catal.*, 1997, **171**, 449-456.

[9] Vit, Z., Portefaix, J.L., Breysse, M., Hydroformylation of ethylene over cobalt, nickel, molybdenum, CoMo and NiMo alumina supported sulfide catalysts. *Appl. Catal. A: Gen.*, 1994, **116**, 259-268.

[10] Zeelie, T.A., Root, A., Krause, A.O.I., Rh/fibre catalyst for ethene hydroformylation: Catalytic activity and characterisation. *Appl. Catal. A: Gen.*, 2005, **285**, 96-109.

[11] Kainulainen, T.A., Niemelä, M.K., Krause, A.O.I., Rh/C catalysts in ethene hydroformylation: the effect of different supports and pretreatments. *J. Mol. Catal. A: Chem.*, 1999, 173-184.

[12] J. Llorca, A.B., G.A. Martin, j. Sales, P. Ramirez de la Piscina, N. Homs, Selective synthesis of alcohols from syngas and hydroformylation of ethylene over supported cluster-derived cobalt catalysts. *Catal. Lett.*, 1996, 87-91.

[13] Gao, J.X., Xu, P.P., Yi, X.D., Wan, H., Tsai, K.R., Hydrogenation and hydroformylation of olefins with water-soluble $Ru_3(CO)_9(TPPMS)_3$ catalys. *J. Mol. Catal. A: Chem.*, 1999, **147**, 99–104.

[14] Ro, I., Xu, M., Graham, G.W., Pan, X., Christopher, P., Synthesis of Heteroatom Rh–ReO_x Atomically Dispersed Species on Al_2O_3 and Their Tunable Catalytic Reactivity in Ethylene Hydroformylation. *ACS Catal.*, 2019, **9**, 10899-10912.

[15] Navidi, N., Thybaut, J.W., Marin, G.B., Experimental investigation of ethylene hydroformylation to propanal on Rh and Co based catalysts. *Appl. Catal. A: Gen.*, 2014, **469**, 357-366.

[16] Xie, Z., Xu, Y., Xie, M., Chen, X., Lee, J.H., Stavitski, E., Kattel, S., Chen, J.G., Reactions of CO_2 and ethane enable CO bond insertion for production of C3 oxygenates. *Nat. Commun.*, 2020, **11**, 1887.

[17] Huang, N., Liu, B., Lan, X., Wang, T., Insights into the bimetallic effects of a RhCo catalyst for ethene hydroformylation: Experimental and DFT investigations. *Ind. Eng. Chem. Res.*, 2020, **59**, 18771-18780.

[18] Huang, L., Xu, Y.D., Guo, W.G., Liu, A.M., Li, D.M., Guo, X.X., Study on Catalysis by Carbonyl Cluster-Derived SiO_2-Supported Rhodium for Ethylene Hydroformylation. *Catal. Lett.*, 1995, **32**, 61-81.

[19] Huang, L., Xu, Y., Synergy of ruthenium and cobalt in SiO_2-supported catalysts on ethylene hydroformylation. *Appl. Catal. A: Gen.*, 2001, **205**, 183–193.

[20] Kainulainen, T.A., Niemelä, M.K., Krause, A.O.I., Ethene hydroformylation on Co/SiO_2 catalysts. *Catal. Lett.*, 1998, 97-101.

[21] Tomishige, K., Furikado, I., Yamagishi, T., Ito, S., Kunimori, K., Promoting effect of Mo on alcohol formation in hydroformylation of propylene and ethylene on $Mo\text{-}Rh/SiO_2$. *Catal. Lett.*, 2005, **103**, 15-21.